Mercury and arsenic mobility in resuspended contaminated estuarine sediments (Asturias, Spain): A laboratory-based study

Efren García-Ordiales [a], Stefano Covelli [b,c,*], Greta Braidotti [b], Elisa Petranich [b], Elena Pavoni [b,d], Alessandro Acquavita [e], Lorena Sanz-Prada [a], Nieves Roqueñí [a], Jorge Loredo [a]

[a] ISYMA Research Group, University of Oviedo, Oviedo, Spain
[b] Department of Mathematics and Geosciences, University of Trieste, Via E. Weiss 2, 34127 Trieste, Italy
[c] CoN.I.S.Ma. Consorzio Nazionale Interuniversitario per le Scienze del Mare, Piazzale Flaminio 9, 00196 Rome, Italy
[d] Department of Chemical and Pharmaceutical Sciences, University of Trieste, Via L. Giorgieri 1, 34127 Trieste, Italy
[e] ARPA FVG Agenzia Regionale per la Protezione Ambientale del Friuli Venezia Giulia, Via Cairoli 14, Palmanova, Udine 33057, Italy

HIGHLIGHTS

- The behaviour of As and Hg species during sediment resuspension was investigated.
- As and Hg occurrence in porewaters is related to dissolution of Fe oxy-hydroxides.
- Particulate and dissolved As and Hg increased following the resuspension.
- Fe oxy-hydroxides strongly regulate the mobility of As and Hg in the water column.
- The restoration of pre-resuspension conditions was mainly reached after few hours.

GRAPHICAL ABSTRACT

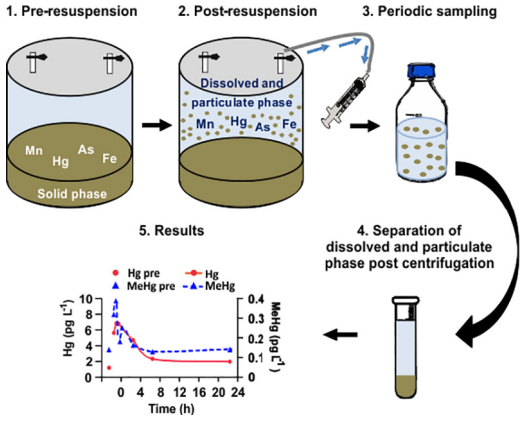

ARTICLE INFO

Article history:
2020 Accepted 8 July 2020

Keywords:
Estuarine sediments
Mercury
Arsenic
Contamination
Resuspension
Dredging

ABSTRACT

Estuarine sediments must be dredged to allow for navigation, and where these sediments are placed after dredging depends upon guidelines based only on the total concentration of contaminants. However, resuspension events could seriously affect the mobility and speciation of contaminants, including potentially toxic trace elements stored in sediments. The effects of resuspension on the cycling of mercury (Hg) and arsenic (As) between the sediment and water column was investigated in a mesocosm study. Four experiments were conducted in three estuaries in northern Spain based on samples collected from sites which have been impacted by decommissioned Hg and As mines and periodically subjected to dredging activities. Designed to mimic the resuspension of particles, each of the experiments revealed that the release of Hg and As species does not only depend on the total concentration in the sediments (16.3–50.9 mg kg^{-1}, for As and 0.52–5.01 mg kg^{-1} for Hg). The contribution from porewaters and the subsequent reductive dissolution and/or desorption appear to be the main processes responsible for the abrupt increase in dissolved Hg and As species (maximum release of 427% and 125%, respectively). In some cases, As and Hg continued to remain at high concentrations in the water column even after the experiments were completed, thus testifying to their critical persistence in the dissolved form. Conversely, at the other sites, the restoration of pre-resuspension conditions was observed only a few hours after resuspension, mainly due to the role of Fe oxy-hydroxides which provides suitable surfaces for adsorption

* Corresponding author at: Department of Mathematics and Geosciences, University of Trieste, Via Weiss, 2, 34128 Trieste, Italy.
E-mail address: covelli@units.it (S. Covelli).

1. Introduction

Estuaries are crucial areas for sediment transfer between fluvial and marine systems, often forming sinks for sediment moving downstream, alongshore or landwards (Ridgway and Shimmield, 2002). A wide range of human activities take place in these sites (i.e., ports, industrial, urban and recreational settlements) and, as a result, estuarine waters receive dissolved and particulate contaminants, including potentially toxic trace elements (PTEs). Fine-grained sediments often become a repository for contaminants by reducing their toxicity (Eggleton and Thomas, 2004 and references therein). However, natural events such as tidal currents, wave action, storm surge and bioturbation (Sanford et al., 1991; Arfi et al., 1993; Kalnejais et al., 2007), along with anthropogenic activities including dredging, shipping and trawling (Schoellhamer, 1996; Lewis et al., 2001), may be responsible for the resuspension of sediment particles. In particular, dredging and disposal are common practices to maintain navigation channels and access to port areas, but they may impact upon aquatic communities (Roberts, 2012) since contaminants can be released in dissolved form in the water column (Stephens et al., 2001; Caplat et al., 2005). When resuspended in the oxic water column, anoxic sediments may result in variable desorption rates of PTEs previously co-precipitated with/or adsorbed to Fe and Mn sulphides (Simpson et al., 1998; Caetano et al., 2003). The released Fe and Mn are quickly reprecipitated, acting as scavengers for PTEs and other contaminants (Caetano et al., 2003; Jones-Lee and Lee, 2005). This precipitation process will involve any particle available with a layer of Fe oxyhydroxide, previously mobilised by the oxidation of sulphides, and PTEs will bind to the newly created adsorption surfaces of the settling particles (Goossens and Zwolsman, 1996). The extent of sediment resuspension and dispersal depends on the water movements in nearby dredging/disposal areas (Eggleton and Thomas, 2004). The modification of the physico-chemical properties (i.e., pH and redox conditions) can affect not only the mobility, but also the bioavailability of toxic compounds with adverse effects on aquatic organisms (Kim et al., 2004, 2006; Cotou et al., 2005; Bocchetti et al., 2008).

Investigation into the potential mobility and bioavailability of contaminants in estuarine sediments is a challenging but essential task, since the understanding of the processes involved in the recycling of these contaminants between solid and aqueous phases may contribute to the preservation of water quality by informing environmental policies. To better evaluate these issues, most research has taken the form of laboratory experiments which simulate the dredging effects using different time intervals (e.g. Van Den Berg et al., 2001; Caetano et al., 2003; Cantwell et al., 2008; Monte et al., 2015; de Freitas et al., 2019).

Among PTEs, mercury (Hg) and arsenic (As) are well known for the recognised toxicity of their different chemical species and diffusion in the environment (i.e., industrial settlements, mining activity). There are several studies on Hg (and methylmercury, MeHg) remobilisation after resuspension from bottom sediments (e.g. Bloom and Lasorsa, 1999; Conaway et al., 2003; Kim et al., 2004; Benoit et al., 2009; Acquavita et al., 2012; Seelen et al., 2018; Zhu et al., 2018). In particular, Bloom and Lasorsa (1999) found that approximately 5% of MeHg bound to the sediment and <1% of total Hg were released during a laboratory mixing experiment, but the release can be limited in quantity and time due to the dilution of the Hg species in the water body and their reburial in the solid phase (Acquavita et al., 2012).

The Asturias coast (northern Spain) represents one of the most impacted regions of Spain due to several anthropogenic activities, including long-term mining of sulphide ore, which have severely affected the Nalòn River drainage basin, the main hydrographical system (3692 km^2) of the region (Loredo et al., 1999; Loredo, 2000; Fernández-Martínez et al., 2005). The sources and distribution of trace elements, especially As and Hg, have been investigated in several environmental matrices including soils, mine tailings, fresh and ground waters and estuarine sediments (e.g. Loredo et al., 2010; Ordóñez et al., 2014; Silva et al., 2014; García-Ordiales et al., 2018). In the Nalón River estuary, in spite of the high levels of As and Hg in the fine sediments, redox conditions appear to govern the speciation cycles of these elements, thus reducing the formation of the most toxic species, such as As(III) and MeHg (García-Ordiales et al., 2018). In addition, there is evidence along the Asturian coasts that other minor estuarine systems may be potentially affected by Hg and As contamination (Forján et al., 2019; García-Ordiales et al., 2019a, 2020; Sanz-Prada et al., 2020).

The primary aim of this research was to investigate the effects of simulated resuspension events in replicate mesocosms to predict the behaviour of Hg and As associated with bottom sediments and porewaters and their fate in the water column after a perturbative event. A comparison among similar estuarine environments in Asturias affected by various sources of contamination and where dredging operations are periodically needed to allow navigation was provided. The occurrence and mobility of Hg and As in this area is of great concern due to their potential bioaccumulation in the aquatic trophic chain. Within the European Union, the Water Framework Directive (WFD, European Parliament, Council of the European Union, 2000) sets "good status" objectives for water bodies throughout the member states. The status is simply based on chemical and ecological criteria. A classification system has been developed to decide upon chemical status, with threshold values known as "Environmental Quality Standards" (EQS). A specific maritime policy was later established and directed for marine ecosystem protection and conservation by the EU Marine Strategy Framework Directive (MSFD) (European Parliament, Council of the European Union, 2008). The MSFD specifically requests that member states implement monitoring programs for the assessment of the environmental status of marine waters. The results of this experimental study may be useful in providing the scientific background to help policy-makers take appropriate decisions regarding dredging and to control PTE contamination levels. This is especially relevant due to the biological richness of estuaries, their significance as sites of a wide variety of food intended for human consumption (fisheries, aquaculture, mussel collection), and the possible implications for the health and economy of affected areas. This experimental approach could be applied to all coastal environments where information regarding the major geochemical processes that regulate PTE behaviour, mobility and fate is needed to support environmental management and risk assessment.

2. Materials and methods

2.1. Study area

The experimental sites are located in three estuaries found in eastern central Asturias (Fig. 1), which has one of the best-preserved coastline environments in Spain. As part of this conservation policy, these estuaries are supported by several environmental protection programs and

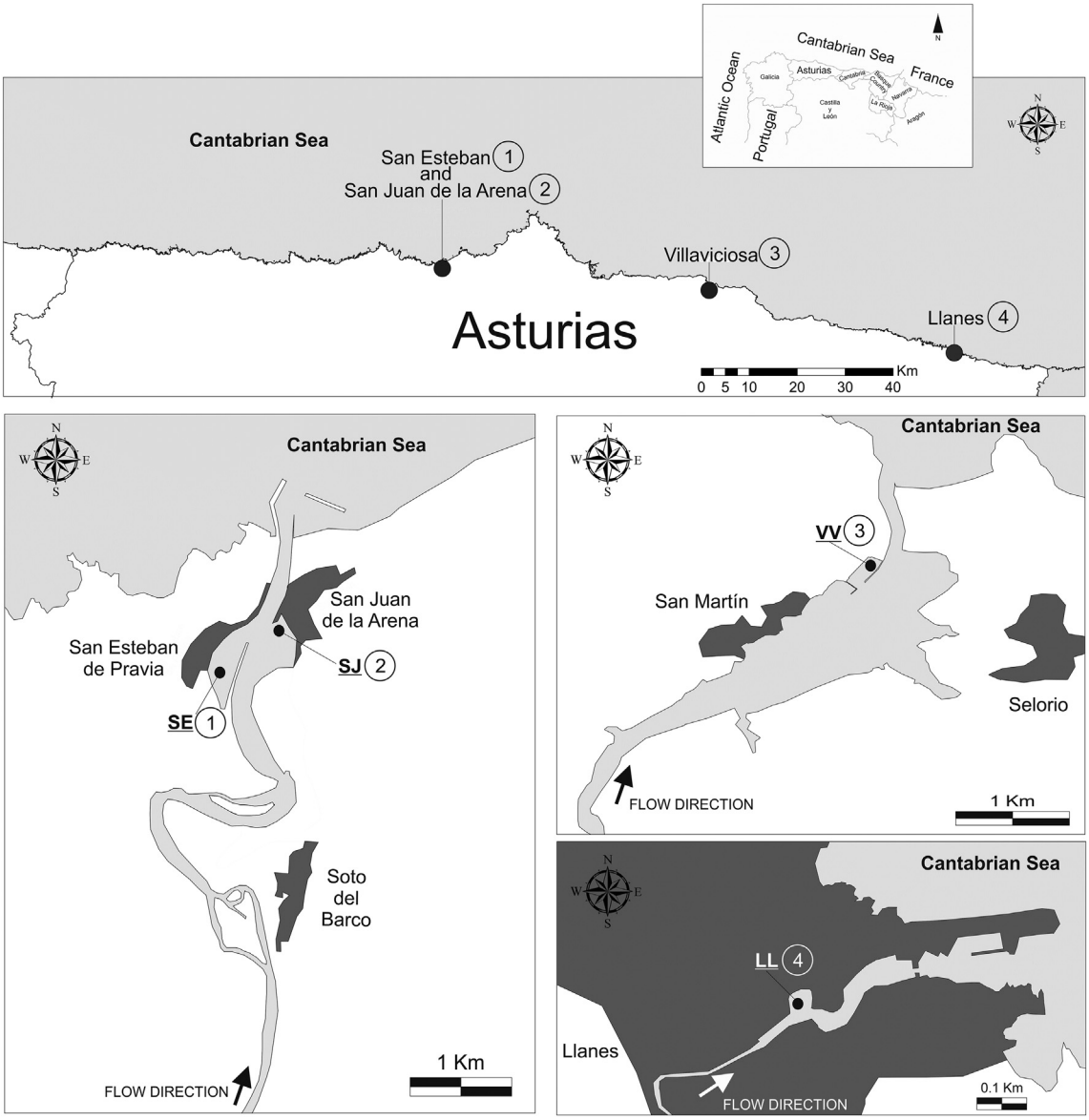

Fig. 1. The study area along the Asturian coast where sediment samples for resuspension experiments were collected from the following sites: the Nalón River Estuary (SJ and SE), the Villaviciosa estuary (VV) and the port of Llanes (LL).

strategic EU initiatives such as the Habitats Directive and the Natura Network 2000 (92/43/EC). Each of these estuaries has diverse characteristics (Table 1).

2.1.1. The Nalón River estuary

The Nalón River empties into the largest drainage basin in the northern Spain. Its estuary has been subject to very high levels of

Table 1
Resuming of the main characteristics of the investigated sampling sites along the Asturian coast: the Nalón River estuary (SJ and SE), the Villaviciosa estuary (VV) and the port of Llanes (LL).

Sampling site		San Juan (SJ)	San Esteban (SE)	Villaviciosa (VV)	Llanes (LL)
Location		Port areas in the Nalón R. estuary		Port area 60 km E of the Nalón R. estuary	Port area 110 km E of the Nalón R. estuary
Latitude		43° 33′ 21.56″ N	43° 33′ 4.90″ N	43° 31′ 31.54″ N	43° 25′13.04″ N
Longitude		6° 4′ 37.51″ W	6° 5′ 40″ W	5° 23′ 21.20″ W	4° 45′12.02″ W
Depth (m)		3.20	4.50	2.40	3.80
Water circulation		Open estuarine area	Sheltered harbour	Sheltered harbour	
Sediment grain size[a]	Sand	26.4%	4.92%	3.91%	27.4%
	Mud	73.6%	95.1%	96.1%	72.6%
As in sediments ($\mu g\ g^{-1}$)		20.1–68.1[b]		Average 11.3[c]	–
Hg in sediments ($\mu g\ g^{-1}$)		0.10–1.33[b]		Average 0.18[c]	>3.81[c]

contamination due to mining which took place over a period of 150 years (García-Ordiales et al., 2019a). The riverine flow to the estuary is high, showing a notable water column stratification that may extend several kilometres (Ceñal and Flor, 1993). The estuary has two port areas which are exposed to the main channel flows, which in turn affects the grain size of the sediments. The San Juan (SJ) port area is quite open and the accumulated bottom sediments are mostly sandy, whereas the San Esteban (SE) port area has a protection dock which acts as a sedimentary trap for silt and clay (García-Ordiales et al., 2018). García-Ordiales et al. (2018, 2019b) reported high concentrations of As (20.1–68.1 μg g^{-1}) and Hg (0.10–1.33 μg g^{-1}) in bottom sediments and the potential transfer to biota.

2.1.2. The Villaviciosa estuary

The Ria de Villaviciosa (VV) is located approximately 60 km east of the Nalón estuary. The drainage basin extends for 160 km^2 and the estuarine area is 12.6 km^2. The freshwater flow rate is low and the tidal influence is strong, producing a total mixing, the absence of water column stratification and a high sedimentary accumulation rate (Flor et al., 1996). Recently, as a consequence of wastewater discharge, mussel collection has been banned. Other potential anthropogenic contamination sources are not known. Conversely, in nearby areas there are different outcrops of bituminous rocks and hydrothermal ores of fluorite that could potentially be the sources of As and Hg (Iglesias and Loredo, 1994; González-Fernández et al., 2018). Preliminary sediment analyses performed by the regional port authority have reported average concentrations of 11.3 μg g^{-1} for As and 0.18 μg g^{-1} for Hg (unpublished data).

2.1.3. The Llanes port

The Llanes (LL) port is approximately 110 km east of the Nalón estuary and 50 km east of VV estuary. Similar to VV, the tidal influence in LL is high, producing a lack of stratification in the water column due to the almost null contributions of freshwater from the inflowing Carroced creek. The sedimentary dynamics are controlled by an access gate between the old (inner) and new (outer) port areas. The tidal flow restriction produced by the gate has converted the old port area, where sediments were collected for this study, into a sedimentary trap of fine sediments similar to SE. Over the last 15 years, sediment monitoring conducted by the regional port authority has shown the presence of high Hg concentrations (up to 3.81 μg g^{-1}) (unpublished data). Potential local sources of Hg are currently under investigation.

2.2. Experimental approach

A scuba diver collected undisturbed short sediment cores by pushing a Plexiglass tube (30 cm length; 16 cm i.d.) into the bottom sediment. Upon collection and transport to the laboratory, these cores were extruded and sectioned into five slices (0–1, 1–2, 2–3.5, 3.5–5 and 5–7 cm) in a N_2-filled chamber to preserve the original redox conditions. At the same time, the redox potential (Eh) was measured in the supernatant water and the corresponding slices. These slices were homogenised and split to determine water content. The remaining sediment was centrifuged at *in situ* temperature and the extracted porewaters, recovered in the inert atmosphere (N_2-filled chamber), were filtered (0.45 μm pore size, i.d. = 33 mm, Millex-HV), collected in acid pre-cleaned vials and stored in a deep-freeze until analyses.

In parallel, bottom sediments and the overlying water were collected by a scuba diver using a cylindrical Plexiglas chamber as a sampler (h = 25 cm, i.d. = 24 cm, wall thickness = 0.6 cm) following the experimental approach applied by Acquavita et al. (2012). The average depth of sediments inside the chamber was 10 cm with approximately 15 cm of overlying water (ratio water/sediment = 1.5). Careful transportation of the chamber to the laboratory minimised perturbation at the sediment-water interface (SWI). Here the overlying water was drained off and carefully replaced with bottom water collected from the same sampling location using a Niskin bottle. This step was taken in order to exclude any possible perturbative effect on the water inside the chamber possibly occurring during transportation (e.g. Bertuzzi et al., 1996; Emili et al., 2011; Acquavita et al., 2012). The basic physico-chemical parameters (T, pH, Eh) were measured using a portable multiprobe (Crison MP41). Redox potential (Eh) measurements were performed by means of a Pt/KCl–Ag/AgCl electrode calibrated with ZoBell solution (220 mV at 25 °C). Values of Eh were not corrected to hydrogen potential.

The simulated resuspension was performed using a mechanical horizontal shaker (130–150 cycles min^{-1}, t = 10 min) after sealing the top hole of the chamber. Periodic sampling of the resulting mixture between dissolved and particulate phases was then performed. In detail, the benthic chamber was left open and undisturbed between one sampling and the next to simulate real environmental conditions where the water column is in direct contact with the atmosphere. In order to allow the collection of water just above the SWI, the cover was repositioned before each sampling. The cover has two valves on its lid, one being connected to a tube (0.5 cm diameter) that allows for water sample collection at approximately 5 cm above the SWI. This is important to properly evaluate variations of the dissolved and particulate concentration of chemical species as a function of time, as well as the grain size composition of the suspended particles which tend to become finer after the resuspension event. Using a plastic syringe, water lying on top of the sediment was syphoned off via one of the two valves on the lid of the chamber and placed in a pre-treated borosilicate container (V_f = 600 mL). Seven samples were recovered within 24 h (T_0 = 0, T_1 = 30 min; T_2 = 1 h; T_3 = 2 h; T_4 = 4 h; T_5 = 8 h; T_6 = 24 h) and the main physico-chemical parameters were promptly measured. Samples were then centrifuged (10,000 rpm min^{-1}, t = 10 min; Eppendorf 5804) to separate the dissolved phase from the suspended particles. The solid fractions were collected for both grain size and chemical analyses. The dissolved phase was subsequently filtered (0.45 μm pore size, i.d. = 33 mm, Millex-HV) and divided for the necessary analytical aliquots.

2.3. Analyses of samples

Grain-size analyses on bottom sediments and resuspended particles were performed following the method outlined by García-Ordiales et al. (2017). The sediment aliquots were oxidised (H_2O_2 = 3%, t = 24 h) to remove most of the organic matter (OM). Successively, the solution was wet-sieved through a 2-mm sieve to remove coarse, shelly fragments. The fraction < 2000 μm was recovered and analysed using a laser diffractometer (Fritsch Anaysette 22 Laser-Particle Sizer Microtec).

The measurement of the isotopic composition of Hg was carried out via gas chromatography combined with inductively coupled plasma mass spectrometry (7890A Agilent GC and HP 7500c Agilent ICP-MS). The determination of the elemental species concentrations was carried out by species-specific isotope dilution mass spectrometry. All sample preparation procedures were previously developed and validated for water (Amouroux et al., 1998; Rodríguez-González et al., 2002; Bouchet et al., 2011) and sediments (Rodríguez Martin-Doimeadios et al., 2003; Rodríguez-González et al., 2007). The mathematical approach of the methods was described in detail in Rodríguez-González et al. (2013).

The As species were analysed using a mobile phase of 2 M phosphate buffered saline (PBS)/0.2 M EDTA (pH 6.0) in a separation column with a 1260 Infinity high-performance liquid chromatograph (HPLC) coupled with ICP-MS. The As species were directly measured in the porewater samples, whereas in the case of solids, 0.1 g of sample was placed together with an extracting agent (1 M H_3PO_4 + 0.1 M, ascorbic acid) in a microwave vessel (Ruiz-Chancho et al., 2005). The digested solution was analysed following the aforementioned method. The accuracy of the results was verified by comparing the total As concentration to the sum of all the determined species concentrations. The recovery of As speciation ranged from 95% to 106%.

Total As, Fe, Mn and S concentrations in dissolved and solid phases (bottom sediments and resuspended sediment particles) were determined by ICP-MS and ICP-OES. For solids, samples were previously

digested by *aqua regia* + HF in a microwave vessel (EPA method 3052). Samples were analysed in batches, and the accuracy of the elemental determination was verified using the CRM042-056 and other internal laboratory standards. Recovery percentages of the different elements were in the range of 93–106%, and the RSD was <7%. The dissolved organic carbon (DOC) was determined using the TOC-V CSH (Shimadzu) instrument.

2.4. Explorative multivariate data analysis

Principal component analysis (PCA) was employed as an unsupervised exploratory chemometric tool for the visual identification of relationships among the samples (PC scores and score plots), within variables (PC loadings and loading plots), and between samples and variables (biplots) (Oliveri et al., 2020). In order to minimise systematic differences between variables, data matrices were pre-processed (column autoscaling) before the multivariate analysis (Oliveri et al., 2019). Multivariate analysis was performed using the CAT (Chemometric Agile Tool) package, based on the R platform (The R Foundation for Statistical Computing, Vienna, Austria) and freely distributed by Gruppo Italiano di Chemiometria (Italy) (Leardi et al., 2019).

3. Results and discussion

3.1. Sediment and porewater chemistry

Grain-size distribution was found to be different among the sampling sites and rather constant with increasing depth (Table 2, Fig. S1A). According to Shepard's (1954) classification, the sediment consisted mostly of silt, which was found to be higher than 90% at VV and SE, followed by SJ and LL which appeared to be less homogeneous with depth. The clayey fraction was rather constant with depth and generally poorly represented, whereas the sandy fraction clearly prevailed at LL and SJ (Table 2, Fig. S1A).

The Asturian estuarine systems are known to be affected by high levels of anthropogenic pressure (García-Ordiales et al., 2018, 2019a, 2019b), thus the sediments collected displayed elevated concentrations of both As and Hg (Table 2). Although disparities in trace element concentrations along the sediment cores collected at the investigated sites are not particularly evident, the PCA output (explaining 84.7% of the total variance) clearly denotes the differences among the various sites which are distinctly represented in the biplot (Fig. S1A). Arsenic was found to be rather homogeneous downcore, with the lone exception being site SE, where As rapidly decreased from 50.9 mg kg^{-1} (0–1 cm) to 31.8 mg kg^{-1} (1–2 cm). No significant differences were observed for Hg at sites VV, SJ and SE (mostly lower than 1.0 mg kg^{-1}), whereas the element was found to be one order of magnitude higher at site LL (3.73 ± 0.76 mg kg^{-1}) as also confirmed in the PCA output showing a relatively clear relationship between Hg and site LL (Fig. S1A). Silva et al. (2014) reported that As incorporated into short-range ordered Fe oxy-hydroxides was the predominant fraction in the stream sediment samples of the Nalòn River drainage basin. This fraction represented >80% of the total As concentration, although realgar and pararealgar [As_4S_4], orpiment [As_2S_3], and arsenic-rich pyrite were the original sulphide ore deposits (Ordóñez et al., 2014).

Similarly, Fe, Mn and S were rather constant moving downcore, except for the weak increase observed for Mn at SE. Comparable S concentrations were found among sites, although slightly higher values were detected at LL and VV. Conversely, Fe and Mn showed the highest concentrations at the Nalón River estuary sites, especially at SE (Fig. S1A).

Estuarine sediments suffer intense chemical, physical and biological reactions due to the interaction between the solid phase and porewaters, promoting the formation of new and altered minerals and/or changes in the porewater composition (Beck et al., 2008; Oliveri et al., 2016). In this context, Fe and Mn oxy-hydroxides represent suitable adsorptive phases for PTEs, especially under oxidising conditions (Turner et al., 2004). Conversely, under conditions of oxygen depletion, Fe and Mn oxy-hydroxides may act as secondary oxidant sources during OM degradation (Froelich et al., 1979) and their subsequent reduction/dissolution could be responsible for the release of dissolved PTEs in porewaters.

Oxidative conditions were found in the supernatant water (Eh ranged from 132 to 161 mV) as well as quite low total dissolved Hg, MeHg and As (III and V) species, followed by Fe and Mn (Fig. 2). This is clearly evident in the PCA output (explaining 71.1% of the total variance) highlighting a strong relationship between the redox conditions and the supernatant water collected from all sites (Fig. S1B). Although some differences occurred among the sites, OM degradation and slow oxygen diffusion through the sediment drove reductive conditions just below the SWI. Redox potential (Eh) decreased downcore at all sites (up to almost −400 mV) whereas dissolved As and Hg species (at LL) and MeHg (0–2 cm) at site SE increased with depth (Figs. 2 and S1B), due to reductive dissolution of Fe oxy-hydroxides (Smedley and Kinniburgh, 2002; Fiket et al., 2019). In detail, the strong correlations between As(III) and As(V) ($r = 0.919$) and between As species and dissolved Fe ($r = 0.770$ and $r = 0.757$ for As(III) and As(V), respectively)

Table 2
Grain size composition, Eh values and concentrations of As, Hg, Mn, Fe and S in the sediment cores collected from the port of Llanes (LL), the Villaviciosa estuary (VV) and the Nalón River Estuary (SJ and SE).

Sampling site	Sediment layer	Sand	Silt	Clay	Eh	As	Hg	Mn	Fe	S
	cm	%	%	%	mV	mg kg^{-1}	mg kg^{-1}	mg kg^{-1}	%	%
LL	0–1	11.8	85.5	2.64	−191	23.9	3.12	101	1.41	1.12
	1–2	33.1	65.5	1.40	−235	23.2	3.29	108	1.50	1.19
	2–3.5	36.8	62.0	1.22	−318	23.0	3.44	109	1.49	1.10
	3.5–5	27.0	71.4	1.58	−341	22.7	3.79	114	1.71	1.40
	5–7	28.1	70.4	1.54	−355	26.3	5.01	124	1.67	1.21
VV	0–1	4.23	93.2	2.54	−153	20.2	0.77	194	2.51	0.81
	1–2	4.06	92.8	3.11	−164	17.6	0.69	190	2.50	0.89
	2–3.5	4.38	92.5	3.07	−175	17.3	0.68	193	2.57	1.01
	3.5–5	2.46	94.4	3.16	−185	16.3	0.57	191	2.57	1.14
	5–7	4.42	92.8	2.81	−191	16.5	0.58	192	2.58	1.20
SJ	0–1	35.8	62.8	1.35	−87	26.8	0.79	411	2.32	1.01
	1–2	32.0	66.6	1.41	−134	25.5	0.58	386	2.37	1.00
	2–3.5	26.3	72.1	1.63	−241	26.1	0.52	447	2.62	0.94
	3.5–5	23.7	74.0	2.32	−187	27.8	0.59	474	2.79	0.97
	5–7	14.1	83.7	2.17	−307	27.3	0.57	469	2.62	0.88
SE	0–1	5.00	92.2	2.78	−118	50.9	0.80	463	3.38	0.62
	1–2	5.01	92.5	2.51	−232	31.8	0.75	499	3.48	0.66
	2–3.5	4.58	92.8	2.61	−263	35.1	0.83	484	3.32	0.84
	3.5–5	4.26	93.0	2.70	−375	32.1	0.67	554	3.03	0.62
	5–7	5.77	91.7	2.51	−348	34.6	0.83	637	3.28	0.82

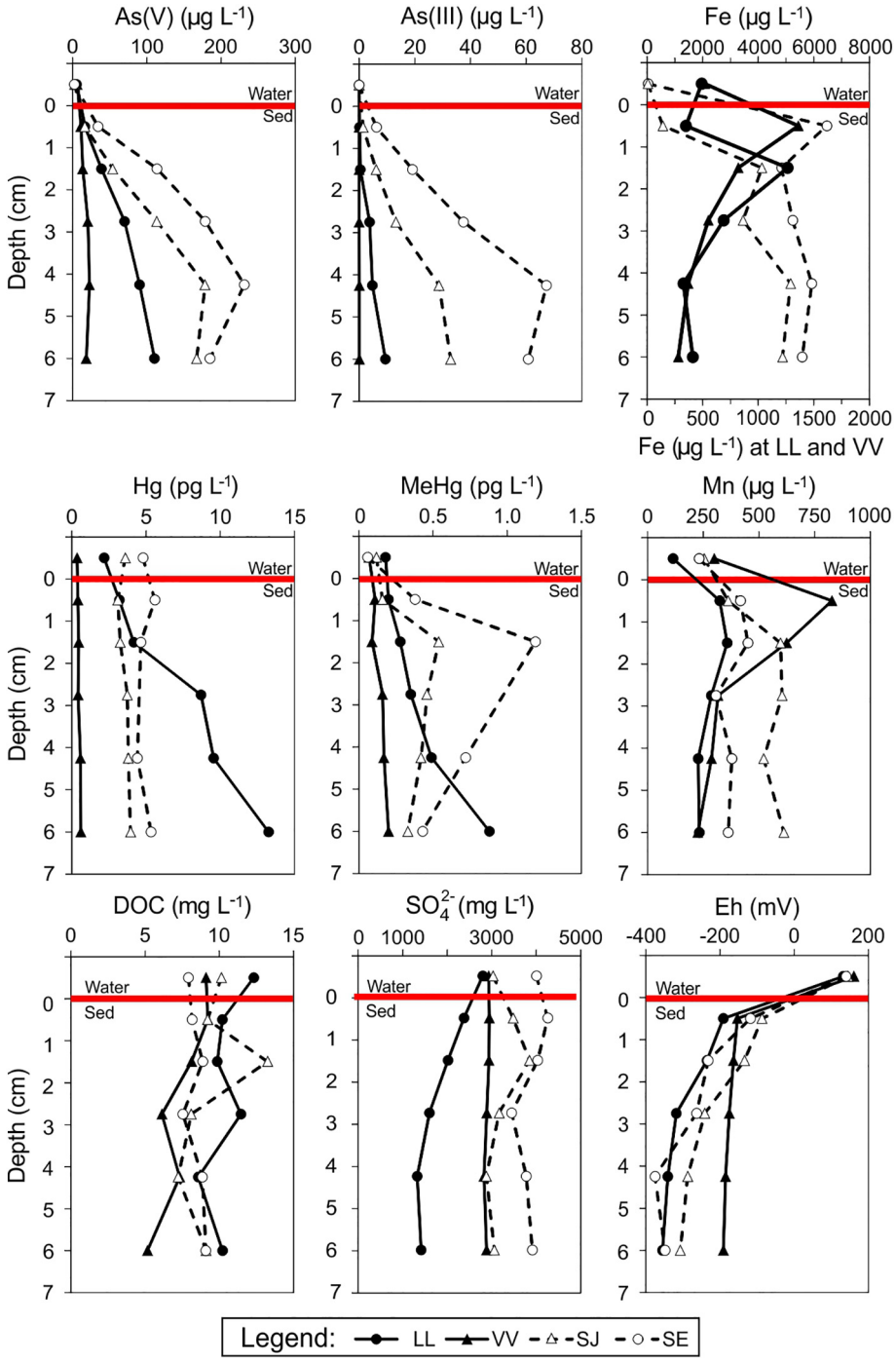

Fig. 2. Vertical profiles for both As and Hg species, Fe, Mn, DOC, SO_4^{2-} in dissolved form in porewaters and Eh values in the four sediment cores collected from the Nalón River estuary (SJ and SE), the Villaviciosa estuary (VV) and the port of Llanes (LL).

highlighted in the PCA output (Fig. S1B) could be explained as Fe dissolution, rather than Mn ($r = 0.171$ and $r = 0.131$ for As(III) and As(V), respectively), drove the release of As species especially at the Nalòn estuary sites (SE and SJ). This is also consistent with the fact that the role of Mn oxide in the reduction and subsequent release of adsorbed As (V) into porewaters definitely appears to be secondary (Masscheleyn et al., 1991) confirming that As should be mainly released from Fe oxy-hydroxides at sites SJ and SE.

Conversely, at site VV, a marked release of dissolved Fe and Mn in the upper sediment (520–1360 µg L^{-1} and 299–828 µg L^{-1}, respectively) appears not to have affected the dissolved Hg and As species that, in fact, showed constant trends with depth (Fig. 2). Moreover, no variability was noticed in the sediments downcore for As, Hg, Fe and Mn. It is possible that their behaviour in the sediment did not result in Fe and Mn oxy-hydroxides precipitation. Due to highly reducing conditions (−400 mV), Hg and As could be present as insoluble or very low soluble sulphur compounds, as also suggested by the strong correlation between Hg and S in the sediment matrix ($r = 0.628$, Fig. S1A) (Fang and Chen, 2015; Wang et al., 2016; Petranich et al., 2018).

Dissolved As species were found to be high in the Nalón estuary (SJ and SE, Fig. S1B), where both As(V) and As(III) notably increased with depth reaching concentrations of 231 and 67.3 µg L^{-1} at SE whereas lower values were found at SJ (179 and 32.9 µg L^{-1}, for As(V) and As (III), respectively). In this context, simultaneous dissolution and

desorption processes involving Fe oxy-hydroxides, carbonate fraction and/or the degradation of OM (Wang et al., 2016 and references therein), may have led to elevated amounts of As(V), which in turn might be rapidly reduced by bacteria to the more labile and toxic As (III) (Dowdle et al., 1996; Smedley and Kinniburgh, 2002; Pfeifle et al., 2018). Indeed, dissolved Fe increased in the first cm (up to 4131 μg L^{-1} at SJ and 6469 μg L^{-1} at SE, respectively) attesting to the transition to anoxic conditions (Fiket et al., 2019). This is in agreement with the trend described for As species, since the reduction of As(V) usually occurred after Fe(III) and before sulphate reduction according to the diagenetic sequence (Froelich et al., 1979; Smedley and Kinniburgh, 2002).

As also confirmed in the PCA output (Fig. S1B), total dissolved Hg gradually increased with depth only at LL (from 2.18 to 13.3 pg L^{-1} in the supernatant water and deepest layer, respectively). In this site, MeHg was found to be extremely low (0.40 ± 0.26 pg L^{-1}) and represented only 8.26 and 6.64% of the dissolved Hg pool in the supernatant water and downcore, respectively. Moreover, a constant increase downcore was observed (from 0.18 to 0.88 pg L^{-1}) whereas slightly elevated amounts of MeHg were found in the 1–2 cm level at sites SJ and SE (Figs. 2 and S1B). Although Hg and MeHg generally displayed extremely low concentrations, the MeHg profile found at site SE suggests that methylation processes mediated by sulphate reducing bacteria (Hines et al., 2017) cannot be completely excluded and could be favoured under low rates of sulphate reduction (Gilmour et al., 1992). The Log K_D of Hg (where K_D is expressed in L kg^{-1}), which describes the partitioning between the solid and dissolved phases (Hammerschmidt et al., 2004), was quite constant with depth, varying between 8.18 ± 0.02 (SE) and 9.13 ± 0.13 (VV), thus suggesting the prevalence of the element in the solid phase (Table S1). The extremely negative values of Eh can favour the occurrence of sulphate reduction allowing for sulphide precipitation (Hines et al., 1997). However, although the highest concentrations of both Hg (5.01 mg kg^{-1}) and S (1.20%) were detected at site LL, no correlation was found between the two elements (r = 0.297 at site LL), contrary to what was observed at sites VV (r = 0.959), SJ (r = 0.577) and SE (r = 0.732). This suggests that the occurrence of Hg at site LL may be related to a different local source currently under investigation. Indeed, Forján et al. (2019) pointed out high concentrations of Hg at Vega beach (approximately 40 km west of site LL) due to the discharge of mine tailings from the district of Berbes which was one of the main fluorite mining areas in Europe where cinnabar was occasionally present (Iglesias and Loredo, 1994; Symons et al., 2017; Levresse et al., 2019). On account of the marine outfall, which has been built up for the discharge since 1990s (Forján et al., 2019), it is reasonable to expect that ocean and shoreline currents play a crucial role in transporting fine suspended particles enriched in Hg into the Llanes estuary (LL).

The sulphate reduction may also have influenced the low levels of dissolved As(III) in the deepest layer at VV and LL (0.07 and 9.42 μg L^{-1}), since the reduction of As(V) is inhibited when sulphate reduction occurs (Moore et al., 1988; Frohne et al., 2011; Burton et al., 2013). At these sites, the reduction of Fe and Mn oxy-hydroxides appear to be relatively notable only in the upper sediments. Conversely, dissolved Fe and Mn showed the highest concentrations in porewaters only below 2 cm at SE and SJ as well as in the corresponding sediment cores (Figs. 2 and 1SB), thus indicating a higher release from sediment to porewaters at the Nalón estuary sites.

Sulphate profiles showed an almost stable trend, except for LL, where they decreased downcore. Together with the increase of Hg and the elevated DOC concentrations, this may have favoured methylation processes at LL, thus explaining the increase in dissolved MeHg in the deeper layers (Figs. 2 and S1B).

3.2. Resuspension experiments

3.2.1. Physico-chemical parameter variability

Total suspended matter (TSM) content was markedly high just after artificial perturbation was stopped (T_0) (Fig. 3), especially at SE and LL (4.88 and 3.42 g L^{-1}, respectively), and decreased abruptly after 30 min (Table S2) at all sites until the end of the experiments. This trend suggests that the effect of resuspension is limited at the initial stage of the experiments, when the highest turbidity was followed by the rapid deposition of the coarser fractions (Van Den Berg et al., 2001).

Total suspended matter (TSM) grain size distribution was determined only at the Nalón estuary (SJ and SE) (Fig. 3). At site SE, coarse and fine silt predominated at T_0, followed by the finer fraction (very fine silt) after 30 min and by the clayey fraction after 8 h. At site SJ, the distribution was trimodal and fine sand, coarse and fine silt prevailed at T_0. Due to the low amount of TSM (close to the lod of the instrument), the distribution was irregular in the rest of the experiment but similar to that described for SE (Fig. 3).

The pH varied in a narrow range at all the sites (7.08–7.86) with the exception of SE (7.04–8.02) (Table S2). The Eh values testified to the occurrence of oxidising conditions throughout all the experiments with a

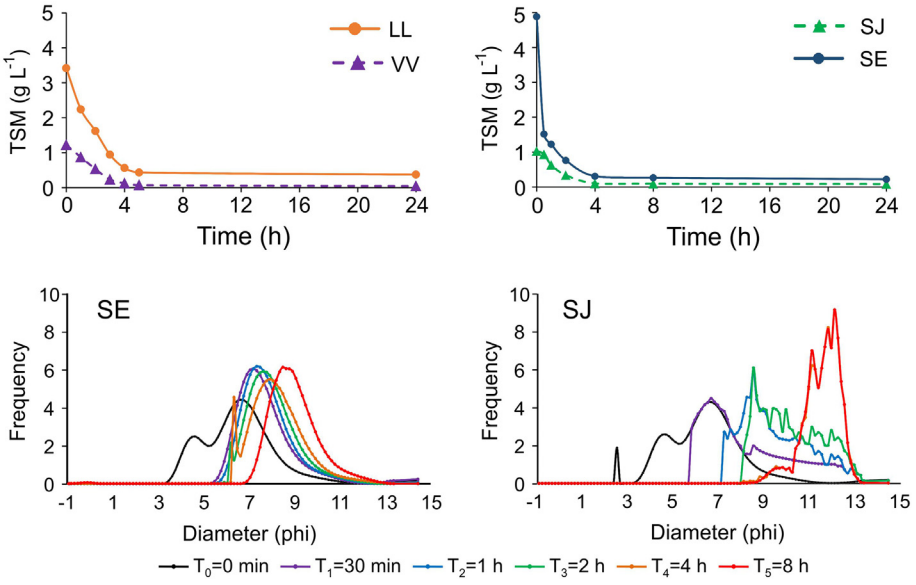

Fig. 3. Trend of total suspended matter (TSM) concentrations during resuspension experiments at all sites (above) and grain-size distribution of TSM at San Esteban (SE) and San Juan (SJ) in the Nalón River Estuary (below).

decreasing trend from pre-resuspension to the initial stage of the experiment (T_0) at LL and SJ, and an increasing trend at VV and SE (Table S2). Generally, there were no marked variations (almost constant) and the values at the end of the experiment were lower than the beginning (Fig. 3). Despite the reductant conditions found in the upper levels of the sediment cores (Fig. 2), the oxidising environment in the mesocosm experiment suggested that the direct contribution from porewaters was negligible (Van Den Berg et al., 2001) or had hidden any dilution processes between porewaters and the water into the chamber.

3.2.2. Behaviour of dissolved chemical species after resuspension

The behaviour of PTEs during a resuspension event is influenced by physico-chemical parameters and by dissolved Fe and Mn occurrence. In oxic conditions, Fe and Mn are present as oxy-hydroxides and are often involved in adsorption processes, co-precipitation, but when reducing conditions occur there is a dissolution with the subsequent release of dissolved PTEs (Gagnon et al., 1997).

Noteworthy differences were found among the sites, both in terms of concentration and trend during the experiments (Figs. 4 and 5). Iron and Mn varied in a wide range being the highest concentrations at SE (up to 7180 and 2760 μg L^{-1}, respectively) followed by SJ. Conversely, at LL and VV there was a low variability and the concentrations were significantly lower.

A common behaviour at all the sites was the increasing trend in the earliest phase of resuspension, since the disturbance events involving anoxic sediments usually lead to the release of dissolved Fe and Mn (Saulnier and Mucci, 2000; Caetano et al., 2003). Considering dissolved Fe, for instance, the maximum concentrations found at SE (7180 μg L^{-1} after 30 min) and SJ (5100 μg L^{-1} at T_0) could be due to the contribution of porewaters following resuspension. In fact, at SE, Fe was found to be higher than 6000 μg L^{-1} in the porewaters extracted from the first centimetre (Fig. 2). Iron and Mn decreased over time at the Nalón estuary sites, reaching concentrations lower than the beginning, most likely due to oxidation processes and subsequent precipitation of Fe oxides. According to Caetano et al. (2003), adsorption and co-precipitation in

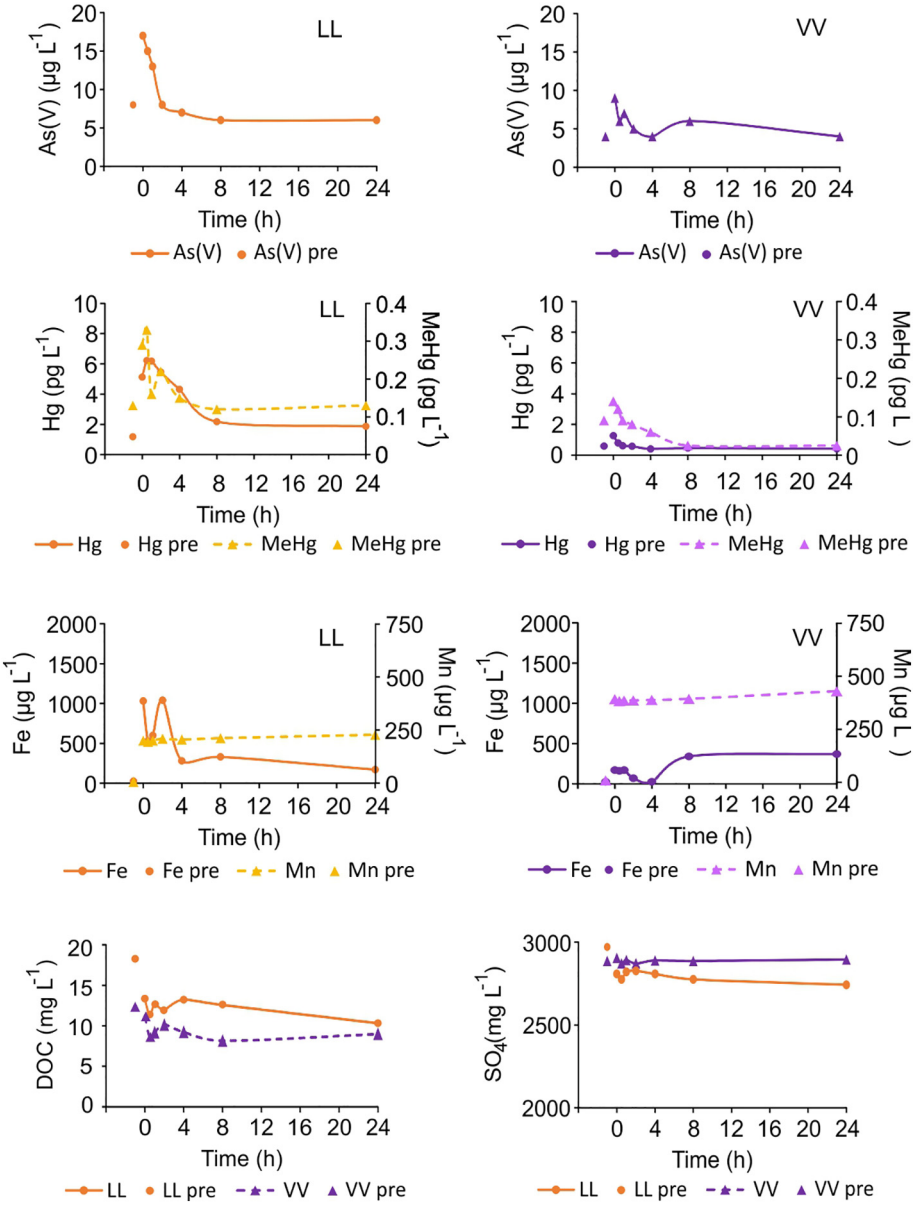

Fig. 4. Behaviour of As(V), As(III), Hg, MeHg, Fe, Mn, DOC and SO_4^{2-} in the dissolved phase of the water column during resuspension experiments at the port of Llanes (LL) and at the Villaviciosa estuary (VV). Note that the term "pre" that follows the chemical element in each graph (e.g. As(V) pre) indicates the PTE concentration before the resuspension event (at time $T_{pre\text{-}res}$).

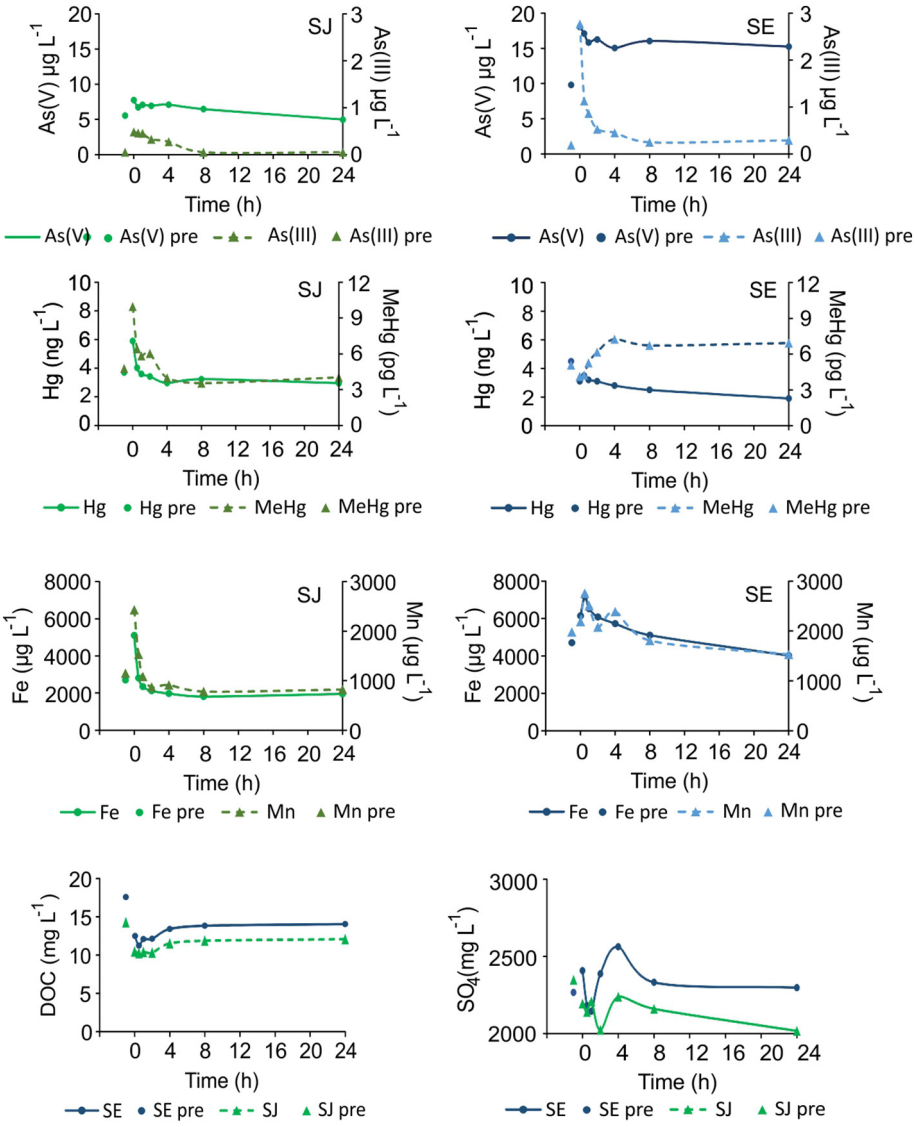

Fig. 5. Behaviour of As(V), As(III), Hg, MeHg, Fe, Mn, DOC and SO_4^{2-} in the dissolved phase of the water column during resuspension experiments at the Nalón River estuary (SJ and SE). Note that Hg, MeHg, Fe and Mn at San Juan (SJ) and San Esteban (SE) show a different scale and As(III) is only present at these two sites. Note that the term "pre" that follows the chemical element in each graph (e.g. As(V) pre) indicates the PTE concentration before the resuspension event (at time $T_{pre\text{-}res}$).

association with Fe oxides represents the main processes responsible for the removal of dissolved Mn from the solution. Indeed, Fe oxides appear to play a crucial role as surface catalysts in the oxidation of Mn (Caetano et al., 2003 and references therein). Indeed, due to the oxidising conditions measured in the chamber (Eh > 120 mV), adsorption and co-precipitation with freshly formed Fe oxides are likely the main processes which remove Mn from the solution.

Conversely, at the other sites, Fe varied more (LL) or less (VV) markedly during the experiments, especially until 4 h (Fig. 4), whereas Mn was almost constant at both sites during the resuspension experiment (24 h). Similar behaviour was observed by Caetano et al. (2003), who stated that following resuspension, dissolved Mn remains in solution over a longer period of time than Fe and then decreases slowly to reach stable levels after one week (Saulnier and Mucci, 2000).

At the four investigated sites, the behaviour of dissolved Hg, MeHg, As (III) and As(V) during the resuspension experiment is discussed in the following paragraphs and described by a negative exponential Eq. (1):

$$C_{Ti} = C_{T0}\, e^{-kx} \quad (1)$$

where C_{Ti} is the concentration at any time (T_i) during the resuspension experiment, C_{T0} is the concentration at T_0 and k is the rate constant for the contaminant dispersion as a function of time (Fig. S2). Eq. (1) was calculated until a decreasing trend was observed and was not applied when the concentration at T_0, was higher than the concentration measured before the resuspension experiment (T_{pre}). Indeed, the final aim was to verify how long it took for the samples to return to their initial pre-resuspension conditions.

3.2.2.1. Behaviour of dissolved mercury species. Although the highest Hg concentrations in sediments and porewaters were found at LL (avg. 3.90 mg kg^{-1} and 6.85 pg L^{-1}, respectively), the release of total dissolved Hg at this site (1.18–6.22 pg L^{-1}) was found to be comparable with those observed at sites SE (1.90–4.50 ng L^{-1}) and SJ (2.95–5.90 ng L^{-1}). The lowest values were found at site VV (0.41–1.27 pg L^{-1}). This could indicate greater Hg mobility at the Nalón estuary sites, in agreement with previous research (García-Ordiales et al., 2018). In addition, MeHg at these sites was found to be twenty times higher (3.54–9.97 pg L^{-1} at SJ and 4.13–6.93 pg L^{-1}at SE, respectively) than

at LL (0.12–0.33 pg L^{-1}) and VV (<lod–0.14 pg L^{-1}) (Figs. 4 and 5). Mercury concentrations at SE and SJ were similar to those reported by Acquavita et al. (2012) in a lagoon environment contaminated by Hg from mining and industrial origin. The same authors reported notably higher (avg. 226 and 51 pg L^{-1}, respectively) MeHg concentrations than our study, likely due to a sudden release from porewaters at T_0.

Total dissolved Hg and MeHg increased after resuspension and then decreased, at all the investigated sites, until the end of the experiment. According to the equation given above (Eq. (1)), dissolved Hg and MeHg reached concentrations comparable to those measured before the resuspension experiment (T_{pre}) after 6 h at sites LL, VV and SJ (Fig. S2). The only exception was the dissolved Hg at site LL, where Hg was found to be slightly higher at the end of the experiment (1.87 pg L^{-1} after 24 h) with respect to the initial stage (1.18 pg L^{-1} before the experiment). These trends are similar to those for dissolved Fe and Mn, thus suggesting a potential removal (scavenging) of Hg species due to Fe oxy-hydroxide formation (Gagnon et al., 1997; Acquavita et al., 2012; Petranich et al., 2018). The only exception was SE, where Hg and MeHg slightly decreased from 4.50 ng L^{-1} and 5.08 pg L^{-1} (pre-resuspension, $T_{pre\text{-}res}$) to 3.10 ng L^{-1} and 4.13 pg L^{-1} (T_0), respectively (Fig. 5). Successively, Hg decreased to the same levels observed at other sites, whereas MeHg progressively increased to 7.25 pg L^{-1} (after 4 h) and remained almost constant until the end of the experiment (after 24 h). This could be attributed both to MeHg released from porewaters (Fig. 2) or to the mobilisation of bioavailable OM during resuspension, which may have favoured the metabolic activity of sulphate-reducing bacteria involved in Hg methylation (Gilmour et al., 1992) as suggested by the high levels of DOC (11.2–17.6 mg L^{-1}, Fig. 5).

Since essential changes in the association with Hg binding phases could influence methylation and the subsequent transfer of MeHg from the sediment to biota (Kim et al., 2006), the MeHg/Hg ratio (%) in the dissolved phase after resuspension was calculated. Despite the low MeHg levels (<lod–0.33 pg L^{-1}), VV and LL displayed the highest average ratio (11.5 and 4.79%, respectively), if compared to SJ and SE (0.15 and 0.22%, respectively). This is due to Hg that was at most one order of magnitude higher than MeHg at LL and VV, whereas at SJ and SE Hg was three orders of magnitude higher. A lower MeHg/Hg ratio was reported by Acquavita et al. (2012) where Hg levels (2.95–15.2 ng L^{-1}) were far higher than MeHg (0.15–0.30 ng L^{-1}): here the ratio increased at the end of the experiment. In our study, this occurred only at SE, where increasing MeHg concentrations and decreasing Hg concentrations over time were observed and could be the result of methylation processes (Fig. 5). Indeed, the MeHg concentrations during resuspension were found to be one order of magnitude higher than those measured in the sediment porewaters, suggesting that a certain amount of MeHg may be produced during the experiment and/or released from the resuspended fine particles due to desorption processes. This is in agreement with previous research at the Nalòn estuary which has found that the highest levels of MeHg in the surface sediments occurred at site SE (García-Ordiales et al., 2018). The same authors also found that low amounts of THg are available for methylation under unperturbed conditions. However, resuspension events may alter the original conditions with the subsequent remobilisation of MeHg from the surface of the resuspended particles. Moreover, at site SE the highest concentrations of inorganic dissolved Hg were observed, as well as elevated concentrations of SO_4^{2-} and an increase in DOC due to OM degradation during the resuspension experiment. Since sediments can show different methylation potential (Bloom et al., 2003) depending on several factors such as bacterial activity, the occurrence of OM and the concentration of inorganic Hg available for methylation (Gilmour et al., 1992; Bloom and Lasorsa, 1999), it is reasonable to hypothesise that sediment resuspension may promote methylation processes at site SE.

3.2.2.2. Behaviour of dissolved arsenic species. The behaviour of As is of particular interest as it was found to be readily bioavailable in surface sediments of the Nalón River estuary (García-Ordiales et al., 2019a, 2019b). The release of As(III) from sediments to porewaters is enhanced under reducing conditions (Bataillard et al., 2014) due to desorption processes (Wilkin and Ford, 2006; Beak et al., 2008). Conversely, As solubility decreases during oxidation events as a result of precipitation of As(V), which often occurs coupled with adsorption on the surface of Fe(III) oxy-hydroxides (Saulnier and Mucci, 2000; Amirbahman et al., 2006; Root et al., 2007; Jeong et al., 2010). Thus, resuspension events involving anoxic sediments strongly affect the release of dissolved As (Saulnier and Mucci, 2000). Indeed, sediment resuspension processes can interfere with the equilibrium of these chemical forms, inducing changes in the redox conditions, which in turn could favour the desorption of As from Fe oxy-hydroxides, as well as the reductive dissolution of these minerals, with a subsequent release from sediment porewaters to the overlying water column (Smedley and Kinniburgh, 2002). This could explain the high As(V) concentrations at T_0, whereas the release of As(III), with concentrations up to ten times lower than As (V), was evident only at SE and SJ (Fig. 5). The prevalence of As (V) may be related to oxidation and/or adsorption processes mediated by Fe oxy-hydroxides, which represent very efficient oxidants of As(III) (Saulnier and Mucci, 2000; Amirbahman et al., 2006; Root et al., 2007; Jeong et al., 2010).

The highest concentrations of As species, released from porewaters, were found at SE. Generally, As(V) markedly decreased at LL and VV reaching pre-resuspension conditions after 4–5 h (Fig. S2). To a lesser extent, something similar was observed at SJ, where As(V) and As(III) concentrations comparable with the beginning (pre-resuspension, $T_{pre\text{-}res}$) were reached after 18 and 9 h for As(V) and As(III), respectively (Fig. S2). On the contrary, the concentration of As(V) at SE after 24 h was higher than that seen before the experiment (15.3 and 9.81 μg L^{-1} at T_6 and $T_{pre\text{-}res}$, respectively). At the same site, As(III) showed a sharp initial increase during the first 30 min of resuspension (0.19 to 2.77 μg L^{-1} at $T_{pre\text{-}res}$ and T_0, respectively) reaching concentrations comparable to those measured before the experiment after 7–8 h, and then decreased over time until the end of the experiment (0.29 μg L^{-1} after 24 h) (Figs. 5 and S2). This behaviour can be attributed to adsorption processes onto Fe oxy-hydroxides (Smedley and Kinniburgh, 2002) (Fig. 5), and to the formation of As(V), which consistently showed high concentrations throughout the experiment as a consequence of As(III) oxidation (Bataillard et al., 2014) sustained by the oxidising conditions measured in the chamber (Table S2). The behaviour of As species during resuspension at site SE was found to be markedly different with respect to the other sites most likely due to the different composition of the sediment and the peculiar characteristics of this port area. Indeed, both sediments and porewaters collected at site SE showed the highest concentrations of As and Fe. Arsenic was found to be notably present in surface sediments of the Nalòn River drainage basin (García-Ordiales et al., 2019a, 2019b) due to intense past mining activity and was found to be mainly associated with Fe oxy-hydroxides (Silva et al., 2014). This is consistent with the results obtained from this study showing that the sediment collected at site SE appeared to be enriched in As with respect to site SJ, most likely due to the presence of a protection dock which acts as a sedimentary trap for fine particles.

On the contrary, the rapid initial decrease in As(V) at LL and VV until 4 h after resuspension, could be due to adsorption processes on Fe oxy-hydroxides (Fig. 4), since dissolved Fe showed comparable behaviour during the experiments. Regarding the As(III), values < lod were likely related to the scarce contribution from porewaters, where very low concentrations were found (0.12–9.42 μg L^{-1} at LL and <lod and 0.07 μg L^{-1} at VV). Moreover, the availability of high concentrations of SO_4^{2-} (>2000 mg L^{-1}) to be reduced can inhibit the reduction of As(V) to As(III) (Burton et al., 2013). Bacterial activity also controls the As(V)/As(III) ratio (Bataillard et al., 2014): in oxic and abiotic conditions the As (V) form prevails, whereas in biotic conditions, As is preserved from total oxidation, thus both chemical forms can be present. This feature deserves to be more carefully investigated and should be taken into consideration in future studies.

Even DOC can be involved in adsorption processes on the suspended particulate matter. In our study, DOC concentrations immediately decreased at T_0, likely caused by the dilution with porewaters, and remained almost constant until 4 h after resuspension. Successively, DOC increased (at VV, SJ and SE) until the end of the experiment (after 24 h) and reached values lower than the beginning, with the exception of LL where a slight decrease was seen between 4 and 24 h after resuspension (13.2 and 10.3 mg L^{-1}, respectively).

3.2.3. Behaviour of the particulate phase after resuspension

Sediment resuspension events can determine the recycling of particles as well as the reintroduction of contaminants into the water column through the SWI (Bloesch, 1995). However, if the event occurred over a short period of time (24 h), the release of dissolved species is limited and most of the PTEs remain bound to the particulate phase (Van Den Berg et al., 2001; Cantwell and Burgess, 2004; Cantwell et al., 2008; Bataillard et al., 2014). According to Guerra et al. (2009), even in heavily contaminated sites (e.g. Pialassa Baiona Lagoon, Italy), dredging does not always have dramatic effects on the environmental quality of the aquatic environment. This could be the case in our study where resuspension was simulated for a limited time.

The Log K_D values for Hg and MeHg (K_D = [PHg] / [DHg], L kg^{-1}) were significantly higher at LL and VV (see Table S3), suggesting that these species remain preferentially partitioned in the particulate phase also during resuspension events, as previously stated by Kim et al. (2004). However, it is interesting to note that Log K_D at SJ and SE showed a decrease of two orders of magnitude if compared to that calculated for core sediments, thus confirming the evidence reported in García-Ordiales et al. (2018). The Log K_D of As species was generally low and did not show noticeable differences among the sites. Conversely, Fe and Mn appeared to be mainly associated with the dissolved phase (Log K_D, 0.81–4.08).

Although Hg and As(V) at SJ (which saw an increase during the first 30 min after resuspension), and As(V) at SE (which saw an increase between 30 min and 1 h after resuspension), particulate PTEs showed decreasing trends at all the sites (Fig. 6). This behaviour was also reported for Zn and Cu by Vidal-Durà et al. (2018) as the result of the settling of the resuspended particles as a function of time.

By comparing the particulate PTE trends with TSM content, a preferential bond to the silty or clayey fraction was found. At SE, the TSM rapidly decreased in the first 4 h after resuspension, from 4.88 (coarse silt) to 0.31 mg L^{-1} (very fine silt), as well as particulate Hg and MeHg, from 14.6 μg g^{-1} and 1.76 pg g^{-1} (T_0) to 5.65 μg g^{-1} and 0.67 pg g^{-1} (after 4 h), respectively. However, as the particles in suspension became finer, particulate Hg and MeHg concentrations slightly increased up to 6.29 μg g^{-1} and 0.83 pg g^{-1} (after 24 h), respectively. This is consistent with the evolution of the grain size spectra and composition as a function of time (Fig. 3) and indicates that Hg and MeHg were bound to both the silty and clayey fractions, in addition to Fe. On the contrary, As(V), As(III) and Mn showed the highest concentrations in the early phase of the experiment, thus were preferentially bound to the silty fraction (Fig. 3).

At SJ, the clay prevailed in suspension as early as 1 h after resuspension, when particulate Hg reached the highest concentration (9.18 μg g^{-1}), and particulate MeHg (0.98 pg g^{-1}) was slightly lower than the beginning (1.29 pg g^{-1}) and decreased as particles settled down (Fig. 6). As observed at site SE, Hg was found to be bound to both grain size fractions, whereas MeHg, Fe and Mn were preferentially bound to the silty fraction. Conversely, particulate As(V) and As(III) increased as the particles in suspension became finer.

3.3. Assessment of arsenic and mercury species released-removal after simulated resuspension events

The amounts of Hg, MeHg, As(V) and As(III) released during the experiments were estimated assuming that the resuspension events involved only the first 3.5 cm of the sedimentary sequence (based on visual observations), considering the size of the chamber and the water content in each layer of the sediment cores. Furthermore, the concentrations at $T_{pre\text{-}res}$ were converted into the amount (mass) of each chemical species. By adding the amounts of elements released by porewaters to those of the water column before resuspension ($T_{pre\text{-}res}$), and dividing by the water volume in the chamber (6.79 L), the chemical species concentrations that should have been found following the resuspension in the water column (T_0) were estimated (Table S4).

The concentrations measured at LL, VV and SJ (only for Hg species promptly re-precipitated/re-adsorbed) at T_0 were higher than those estimated for the sole porewater contribution, thus there was also an active desorption from the resuspended sediment. For the Nalón River estuary, the concentrations of Hg and As species at T_0 were found to

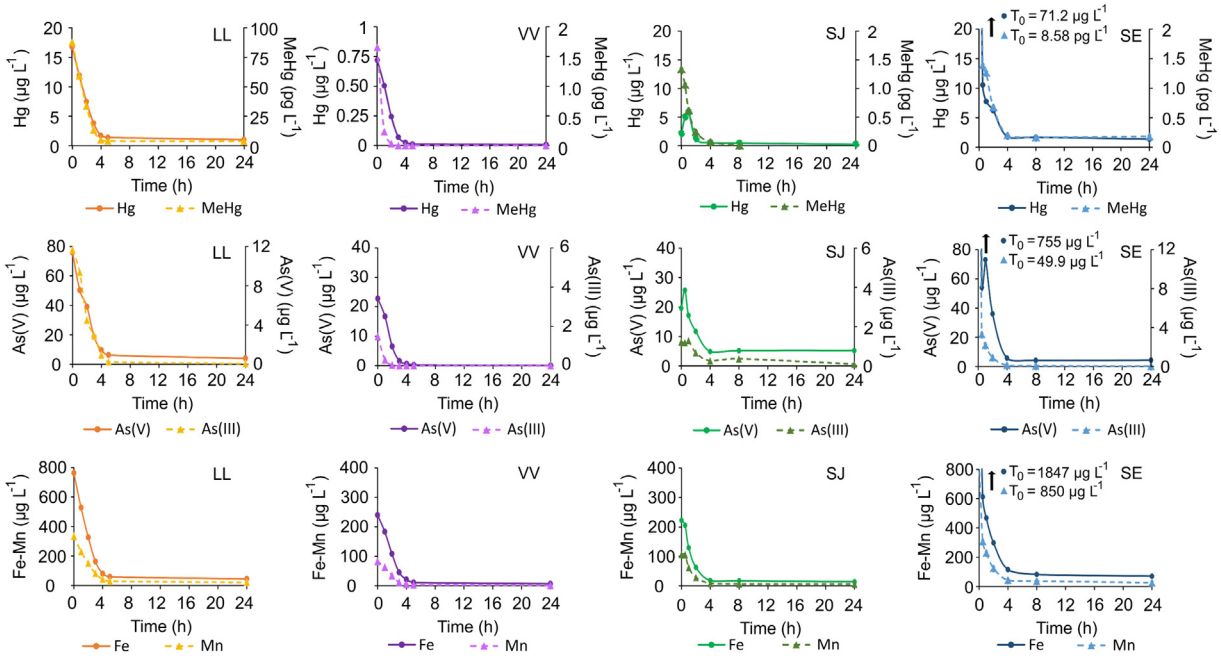

Fig. 6. Behaviour of As(V), As(III), Hg, MeHg, Fe and Mn in the particulate phase of the water column during resuspension experiments at all investigated sites, expressed using different scales.

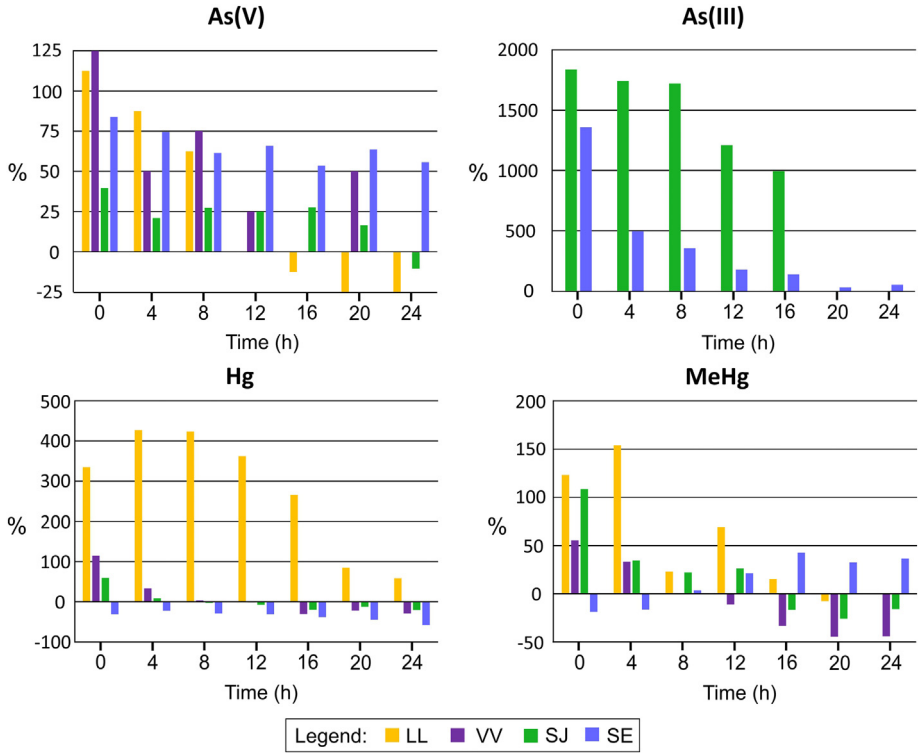

Fig. 7. Percentages of removal (negative values) and/or release (positive values) of As and Hg species in the water column from T_0 to T_6 with respect to the dissolved concentrations before resuspension ($T_{pre\text{-}res}$).

be lower than the estimated concentrations at SE. In addition, the percentages of As and Hg species in the water column until the end of the experiment (after 24 h), with respect to the dissolved concentrations before resuspension were calculated (Table S4 and Fig. 7). Positive values for Hg and MeHg (excluding the sampling performed after 8 h) at LL and, in the first hour, at VV, suggested a further release from resuspended sediments. In detail, at LL the percentage of Hg released at T_0 was especially high (335%) and remained so (58%) after 24 h. Surprisingly, a scarce release at T_0 was found at SE where the concentration was approximately 30% lower than before the experiment ($T_{pre\text{-}res}$) and became even lower (−58%) after 24 h (Fig. 7). The time of removal for MeHg from the water column was quite variable among the sites, however, the MeHg levels were almost constant thus suggesting the enhancement of methylation processes after resuspension as observed by Acquavita et al. (2012). As suggested by Bloom and Lasorsa (1999), the mixing of surface sediments associated with fresh sulphate and organic carbon with contaminated deep sediments may be a favourable environment for MeHg production: if these conditions occur, unacceptably high levels of MeHg could result, however, this does not appear to be the case in this study.

At the end of the experiment, the concentration of As(V) at site SJ (4.97 μg L^{-1}) was found to be slightly lower than that measured before the resuspension (5.55 μg L^{-1}, $T_{pre\text{-}res}$) suggesting that the As (V) released during resuspension was removed at the end of the experiment (after 24 h). On the contrary, this was not evident at site SE, where As(V) concentration was still higher (56%) at the end of the experiment (15.5 μg L^{-1}) than before the experiment (9.81 μg L^{-1}, $T_{pre\text{-}res}$). Something similar was observed for As(III) which was removed after 9 h at SJ (<lod) and slightly higher (0.29 μg L^{-1} after 24 h) than before resuspension (0.19 μg L^{-1}, $T_{pre\text{-}res}$) at SE.

4. Conclusions

Mainly due to the legacy of mining activities, Hg and As accumulated in sediments found on the Asturian coasts could be problematic in the case of resuspension due to natural (e.g. storm surges) or anthropogenic events (e.g. dredging). A preliminary characterisation of the area (sediment cores) was provided for the selected sites. Furthermore, to investigate the effect of resuspension and the subsequent remobilisation and redistribution of As and Hg species, a mesocosm experiment (simulated resuspension under controlled conditions) was performed. The major findings can be summarised as follows:

- The bottom sediments were mostly constituted of silt at SE and VV, whereas sand prevailed at LL and SJ. Arsenic concentration demonstrated a wider range than Hg moving downcore with rather homogeneous profiles. However, for both elements the levels were quite high and exceeded the standard set by the EU. Increasing negative Eh values moving downcore were measured at all the sites.
- Several dissolved species were determined in porewaters (As(V), As (III), Hg and MeHg). Generally, Hg concentrations were rather constant with depth. In the case of As species, an increase due to the dissolution and desorption from Fe, rather than Mn, oxy-hydroxides coupled with the transition from oxic to anoxic conditions occurred. These processes could have led to high amounts of As(V), which in turn might be rapidly reduced to the more labile and toxic As(III). The highest As(V) and SO_4^{2-} concentrations detected in porewaters at the Nalón River estuarine sites could testify to a scarce sulphate reduction which usually inhibits the reduction of As(V). Moreover, the low rates of sulphate reduction could also explain the pronounced increase in MeHg at the same sites (SJ and SE).
- Particulate and dissolved PTE concentration increased when the artificial perturbation stopped and together TSM rapidly decreased over time. The abrupt increase in dissolved PTEs can be mainly ascribed to the porewater contribution and the effects of resuspension lasted only a few hours until pre-resuspension conditions were restored. Part of the Hg and MeHg released from porewaters and/or desorbed during resuspension was removed after 6 h at sites LL, VV and SJ (with the exception of Hg at site LL) by the re-adsorption onto the settling fine particles and/or co-precipitation with Fe oxy-hydroxides. In the case of As species, the restoration of the pre-resuspension

concentrations of As(III) was reached after 7–9 h at the Nalòn estuary sites. Something similar was observed for As(V) which showed concentrations comparable to the beginning after 4–5 h at LL and VV and after 18 h at SJ, whereas the re-adsorption and/or re-precipitation was incomplete at site SE.

These results suggest that resuspension events of contaminated estuarine sediments can be critical for the surrounding environment, resulting in a worsening of the quality for water and biota. The consequences, however, are not unequivocal, strongly depending on site characteristics and, as seen in the mesocosm experiments, appear to be limited in time. The restoration of pre-resuspension conditions is observed a few hours after resuspension, but in some sites precautions should be taken when planning to dredge. Indeed, at the Nalòn estuary and in particular at site SE, the release of dissolved As(V) and MeHg appeared to be favoured during resuspension and can be considered an important issue to be taken into account when dredging must be done.

Further investigation could be helpful in order to elucidate the behaviour of other pollutants such as POPs and TBT, which commonly affect estuarine and coastal areas. Moreover, it would be useful to monitor the water column quality during dredging operations *in situ* and to compare the results with the mesocosm approach.

CRediT authorship contribution statement

Efren García-Ordiales: Conceptualization, Methodology, Formal analysis, Investigation, Data curation, Writing - original draft, Supervision. **Stefano Covelli:** Conceptualization, Methodology, Formal analysis, Investigation, Writing - original draft, Visualization, Writing - review & editing. **Greta Braidotti:** Methodology, Investigation, Resources. **Elisa Petranich:** Investigation, Writing - original draft, Visualization, Writing - review & editing. **Elena Pavoni:** Formal analysis, Visualization, Investigation, Resources, Writing - original draft, Writing - review & editing. **Alessandro Acquavita:** Investigation, Writing - original draft. **Lorena Sanz-Prada:** Methodology, Investigation, Resources. **Nieves Roqueñí:** Supervision, Project administration. **Jorge Loredo:** Supervision, Project administration.

Declaration of competing interest

The authors declare that they have no known competing financial interests or personal relationships that could have appeared to influence the work reported in this paper.

Acknowledgments

This study was co-supported by the Spanish Ministry of Economy, Industry and Competitiveness through the Research Projects METRAMER [grant number: MINECO-13-CGL2013-44980-R] and ECOMER [grant number: MINECO-18-CGL2017-84268-R] and the Asturias Ministry of Education and Science [grant number: FC-15-GRUPIN14-067]. The authors are very grateful to José Manuel Rico for his valuable support in sampling operations. Karry Close is warmly acknowledged for proofreading the manuscript. The anonymous reviewers are sincerely acknowledged for their critical reviews and useful suggestions which improved the quality of the manuscript.

References

Acquavita, A., Covelli, S., Emili, A., Berto, D., Faganeli, J., Giani, M., Horvat, M., Koron, N., Rampazzo, F., 2012. Mercury in the sediments of the Marano and Grado Lagoon (northern Adriatic Sea): sources, distribution and speciation. Estuar. Coast. Shelf S. 113, 20–31.

Amirbahman, A., Kent, D.B., Curtis, G.P., Davis, J.A., 2006. Kinetics of sorption and abiotic oxidation of arsenic(III) by aquifer materials. Geochim. Cosmochim. Ac. 70, 533–547.

Amouroux, D., Tessier, E., Pécheyran, C., Donard, O.F.X., 1998. Sampling and probing volatile metal(loid) species in natural waters by in-situ purge and cryogenic trapping followed by gas chromatography and inductively coupled plasma mass spectrometry (P-CT-GC-ICP/MS). Anal. Chim. Acta 377, 241–254.

Arfi, R., Guiral, D., Bouvy, M., 1993. Wind induced resuspension in a shallow tropical lagoon. Estuar. Coast. Shelf S. 36, 587–604.

Bataillard, P., Grangeon, S., Quinn, P., Mosselmans, F., Lahfid, A., Wille, G., Joulian, C., Battaglia-Brunet, F., 2014. Iron and arsenic speciation in marine sediments undergoing a resuspension event: the impact of biotic activity. J. Soils Sediments 14, 615–629.

Beak, D.G., Wilkin, R.T., Ford, R.G., Kelly, S.D., 2008. Examination of arsenic speciation in sulfidic solutions using X-ray absorption spectroscopy. Environ. Sci. Technol. 42, 1643–1650.

Beck, M., Dellwig, O., Schnetger, B., Brumsack, H.J., 2008. Cycling of trace metals (Mn, Fe, Mo, U, V, Cr) in deep pore waters of intertidal flat sediments. Geochim. Cosmochim. Ac. 72, 2822–2840.

Benoit, J.M., Shull, D.H., Harvey, R.M., Beal, S.A., 2009. Effect of bioirrigation on sediment-water exchange of methylmercury in Boston Harbor, Massachusetts. Environ. Sci. Technol. 43, 3669–3674.

Bertuzzi, A., Faganeli, J., Brambati, A., 1996. Annual variation of benthic nutrient fluxes in shallow coastal waters (Gulf of Trieste, northern Adriatic Sea). Mar. Ecol. 17, 261–278.

Bloesch, J., 1995. Mechanisms, measurement and importance of sediment resuspension in lakes. Mar. Freshw. Res. 46, 295–304.

Bloom, N.S., Lasorsa, B.K., 1999. Changes in mercury speciation and the release of methyl mercury as a result of marine sediment dredging activities. Sci. Total Environ. 237–238, 379–385.

Bloom, N.S., Preus, E., Katon, J., Hiltner, M., 2003. Selective extractions to assess the biogeochemically relevant fractionation of inorganic mercury in sediments and soils. Anal. Chim. Acta 479, 233–248.

Bocchetti, R., Fattorini, D., Pisanelli, B., Macchia, S., Oliviero, L., Pilato, F., Pellegrini, D., Regoli, F., 2008. Contaminant accumulation and biomarker responses in caged mussels, *Mytilus galloprovincialis*, to evaluate bioavailability and toxicological effects of remobilized chemicals during dredging and disposal operations in harbours areas. Aquat. Toxicol. 89, 257–266.

Bouchet, S., Tessier, E., Monperrus, M., Bridou, R., Clavier, J., Thouzea, G., Amouroux, D., 2011. Measurements of gaseous mercury exchanges at the sediment–water, water–atmosphere and sediment–atmosphere interfaces of a tidal environment (Arcachon Bay, France). J. Environ. Monitor. 13, 1351–1359.

Burton, E.D., Johnston, S.G., Kraal, P., Bush, R.T., Claff, S., 2013. Sulfate availability drives divergent evolution of arsenic speciation during microbially mediated reductive transformation of schwertmannite. Environ. Sci. Technol. 47, 2221–2229.

Caetano, M., Madureira, M.J., Vale, C., 2003. Metal remobilisation during resuspension of anoxic contaminated sediment: short-term laboratory study. Water Air Soil Pollut. 143, 23–40.

Cantwell, M.G., Burgess, R.M., 2004. Variability of parameters measured during the resuspension of sediments with a particle entrainment simulator. Chemosphere 56, 51–58.

Cantwell, M.G., Burgess, R.M., King, J.W., 2008. Resuspension of contaminated field and formulated reference sediments. Part I: evaluation of metal release under controlled laboratory conditions. Chemosphere 73, 1824–1831.

Caplat, C., Texier, H., Barillier, D., Lelievre, C., 2005. Heavy metals mobility in harbour contaminated sediments: the case of Port-en-Bessin. Mar. Pollut. Bull. 50, 504–511.

Ceñal, R.C., Flor, G., 1993. Evolución reciente del estuario del Nalón (Asturias). Cuaternario y Geomorfología 7, 23–34.

Conaway, C.H., Squire, S., Mason, R.P., Flegal, A.R., 2003. Mercury speciation in the San Francisco Bay estuary. Mar. Chem. 80, 199–225.

Cotou, E., Gremare, A., Charles, F., Hatzianestis, I., Sklivagou, E., 2005. Potential toxicity of resuspended particulate matter and sediments: environmental samples from the Bay of Banyuls-sur-Mer and Thermaikos Gulf. Cont. Shelf Res. 25, 2521–2532.

de Freitas, A.R., de Castro Rodrigues, A.P., Monte, C.N., Freire, A.S., Santelli, R.E., Machado, W., Sabadini-Santos, E., 2019. Increase in the bioavailability of trace metals after sediment resuspension. SN Applied Sciences 1, 1288. https://doi.org/10.1007/s42452-019-1276-8.

Dowdle, P.R., Laverman, A.M., Oremland, R.S., 1996. Bacterial dissimilatory reduction of arsenic (V) to arsenic (III) in anoxic sediments. Appl. Environ. Microbiol. 62, 1664–1669.

Eggleton, J., Thomas, K.V., 2004. A review of factors affecting the release and bioavailability of contaminants during sediment disturbance events. Environ. Int. 30, 973–980.

Emili, A., Koron, N., Covelli, S., Faganeli, J., Acquavita, A., Predonzani, S., De Vittor, C., 2011. Does anoxia affect mercury cycling at the sediment-water interface in the Gulf of Trieste (northern Adriatic Sea)? Incubation experiments using benthic flux chambers. Appl. Geochem. 26, 194–204.

European Parliament, Council of the European Union, 2000. Water Framework Directive. 2000/60/EC.

European Parliament, Council of the European Union, 2008. Establishing a Framework for Community Action in the Field of Marine Environmental Policy (Marine Strategy Framework Directive). 2008/56/EC.

Fang, T.H., Chen, Y.S., 2015. Arsenic speciation and diffusion flux in Danshuei Estuary sediments, Northern Taiwan. Mar. Pollut. Bull. 101, 98–109.

Fernández-Martínez, R., Loredo, J., Ordóñez, A., Rucandio, M.I., 2005. Distribution and mobility of mercury in soils from an old mining area in Mieres, Asturias (Spain). Sci. Total Environ. 346, 200–212.

Fiket, Ž., Fiket, T., Ivanić, M., Mikac, N., Kniewald, G., 2019. Pore water geochemistry and diagenesis of estuary sediments – an example of the Zrmanja River estuary (Adriatic coast, Croatia). J. Soils Sediments 19, 2048–2060.

Flor, G., Fernández Pérez, L.A., Menéndez Fidalgo, R., Martínez Cueto-Felgueroso, E.M., Rodríguez Casero, G., 1996. Dynamics and sedimentation of the mesotidal estuary of Villaviciosa (Asturias, Northern Spain). Rev. Soc. Geol. Esp. 9, 3–4.
Forján, R., Baragaño, D., Boente, C., Fernández-Iglesias, E., Rodríguez-Valdes, E., Gallego, J.R., 2019. Contribution of fluorite mining waste to mercury contamination in coastal systems. Mar. Pollut. Bull. 149, 110576.
Froelich, P.N., Klinkhammer, G.P., Bender, M.L., Luedtke, N.A., Heath, G.R., Cullen, D., Dauphin, P., Hammond, D., Hartman, B., Maynard, V., 1979. Early oxidation of organic matter in pelagic sediments of the eastern equatorial Atlantic: suboxic diagenesis. Geochim. Cosmochim. Ac. 43, 1075–1090.
Frohne, T., Rinklebe, J., Diaz-Bone, R.A., Du Laing, G., 2011. Controlled variation of redox conditions in a floodplain soil: impact on metal mobilization and biomethylation of arsenic and antimony. Geoderma 160, 414–424.
Gagnon, C., Pelletier, E., Mucci, A., 1997. Behaviour of anthropogenic mercury in coastal marine sediments. Mar. Chem. 59, 159–176.
García-Ordiales, E., Loredo, J., Covelli, S., Esbrí, J.M., Millán, R., Higueras, P., 2017. Trace metal pollution in freshwater sediments of the world's largest mercury mining district: sources, spatial distribution, and environmental implications. J. Soils Sediments 17, 1893–1904.
García-Ordiales, E., Covelli, S., Rico, J.M., Roqueñí, N., Fontolan, G., Flor-Blanco, G., Cienfuegos, P., Loredo, J., 2018. Occurrence and speciation of arsenic and mercury in estuarine sediments affected by mining activities (Asturias, northern Spain). Chemosphere 198, 281–289.
García-Ordiales, E., Cienfuegos, P., Roqueñí, N., Covelli, S., Flor-Blanco, G., Fontolan, G., Loredo, J., 2019a. Historical accumulation of potentially toxic trace elements resulting from mining activities in estuarine salt marshes sediments of the Asturias coastline (northern Spain). Environ. Sci. Pollut. Res. 26, 3115–3128.
García-Ordiales, E., Roqueñí, N., Rico, J.M., Cienfuegos, P., Alvarez, R., Ordóñez, A., 2019b. Assessment of the toxicity toward Vibrio fischeri in sediments of a mining impacted estuary in the north of Spain. Sci. Total Environ. 660, 826–833.
García-Ordiales, E., Flor-Blanco, G., Roqueñí, N., Covelli, S., Cienfuegos, P., Fontolan, G., Loredo, J., 2020. Anthropocene human footprint in the Nalón estuarine sediments (northern Spain). Mar. Geol. 424, 106167.
Gilmour, C.C., Henry, E.A., Ralph, M., 1992. Sulfate stimulation of mercury methylation in freshwater sediments. Environ. Sci. Technol. 26, 2281–2287.
González-Fernández, B., Rodríguez-Valdés, E., Gallego, J.R., 2018. Contaminación de un acuífero por metales pesados de origen geogénico: importancia del control geológico e hidrogeológico de los sondeos de captación de aguas. Geogaceta 64, 59–62.
Goossens, H., Zwolsman, J.J.G., 1996. An evaluation of the behaviour of pollutants during dredging activities. Terra et Aqua 62, 20–28.
Guerra, R., Pasteris, A., Ponti, M., 2009. Impacts of maintenance channel dredging in a northern Adriatic coastal lagoon. I: effects on sediment properties, contamination and toxicity. Estuar. Coast. Shelf S. 85, 134–142.
Hammerschmidt, C.R., Fitzgerald, W.F., Lamborg, C.H., Balcom, P.H., Visscher, P.T., 2004. Biogeochemistry of methylmercury in sediments of Long Island Sound. Mar. Chem. 90, 31–52.
Hines, M.E., Faganeli, J., Planinc, R., 1997. Sedimentary anaerobic microbial biogeochemistry in the Gulf of Trieste, Northern Adriatic Sea: influences of bottom water oxygen depletion. Biogeochemistry 39, 65–86.
Hines, M.E., Covelli, S., Faganeli, J., Horvat, M., 2017. Controls on microbial mercury transformations in contaminated sediments downstream of the Idrija mercury mine (West Slovenia) to the Gulf of Trieste (northern Adriatic). J. Soils Sediments 17, 1961–1971.
Iglesias, J.G., Loredo, J., 1994. Geological, geochemical and mineralogical characteristics of the Asturias Fluorspar District, Northern Spain. Explor. Min. Geol. 3, 31–37.
Jeong, H.Y., Han, Y.S., Park, S.W., Hayes, K.F., 2010. Aerobic oxidation of mackinawite (FeS) and its environmental implication for arsenic mobilization. Geochim. Cosmochim. Ac. 74, 3182–3198.
Jones-Lee, A., Lee, G.F., 2005. Role of iron chemistry in controlling the release of pollutants from resuspended sediments. Remediation 16, 33–41.
Kalnejais, L.H., Martin, W.R., Signell, R.P., Bothner, M.H., 2007. Role of sediment resuspension in the remobilization of particulate-phase metals from coastal sediments. Environ. Sci. Technol. 41, 2282–2288.
Kim, E.H., Mason, R.P., Porter, E.T., Soulen, H.L., 2004. The effect of resuspension on the fate of total mercury and methylmercury in a shallow estuarine ecosystem: a mesocosm study. Mar. Chem. 86, 121–137.
Kim, E.H., Mason, R.P., Porter, E.T., Soulen, H.L., 2006. The impact of resuspension on sediment mercury dynamics, and methylmercury production and fate: a mesocosm study. Mar. Chem. 102, 300–315.
Leardi, R., Melzi, C., Polotti, G., 2019. CAT (Chemometric Agile Tool). freely downloadable from. http://gruppochemiometria.it/index.php/software. (Accessed 3 September 2019). .
Levresse, G., Tritlla, J., Rosique, A.R., Cardellach, E., Rollion-Bard, C., Pironon, J., Sandoval, S.J., 2019. Hydrocarbons in silica: PVTX properties of fluids and the genesis of diamond quartz from Caravia-Berbes Fluorite district (Asturias, Spain). Mar. Petrol. Geol. 102, 1–15.
Lewis, M.A., Weber, D.E., Stanley, R.S., Moore, J.C., 2001. Dredging impact on an urbanized Florida bayou: effects on benthos and algal-periphyton. Environ. Pollut. 115, 161–171.
Loredo, J., 2000. Historic Unreclaimed Mercury Mines in Asturias (Northwestern Spain): Environmental Approaches. Assessing and Managing Mercury From Historic and Current Mining Activities. pp. 175–180.
Loredo, J., Ordóñez, A., Gallego, J., Baldo, C., Garcia-Iglesias, J., 1999. Geochemical characterisation of mercury mining spoil heaps in the area of Mieres (Asturias, northern Spain). J. Geochem. Explor. 67, 377–390.
Loredo, J., Petit-Domínguez, M.D., Ordóñez, A., Galán, M.P., Fernández-Martínez, R., Alvarez, R., Rucandio, M.I., 2010. Surface water monitoring in the mercury mining district of Asturias (Spain). J. Hazard. Mater. 176, 323–332.
Masscheleyn, P.H., Delaune, R.D., Patrick Jr., W.H., 1991. Arsenic and selenium chemistry as affected by sediment redox potential and pH. J. Environ. Qual. 20, 522–527.
Monte, C.N., Rodrigues, A.P.C., Cordeiro, R.C., Freire, A.S., Santelli, R.E., Machado, W., 2015. Changes in Cd and Zn bioavailability upon an experimental resuspension of highly contaminated coastal sediments from a tropical estuary. Sustain. Water Resour. Manag. 1, 335–342.
Moore, J.N., Ficklin, W.H., Johns, C., 1988. Partitioning of arsenic and metals in reducing sulfidic sediments. Environ. Sci. Technol. 22, 432–437.
Oliveri, E., Salvagio Manta, D., Bonsignore, M., Cappello, S., Tranchida, G., Bagnato, E., Sabatino, N., Santisi, S., Sprovieri, M., 2016. Mobility of mercury in contaminated marine sediments: biogeochemical pathways. Mar. Chem. 186, 1–10.
Oliveri, P., Malegori, C., Simonetti, R., Casale, M., 2019. The impact of signal pre-processing on the final interpretation of analytical outcomes – a tutorial. Anal. Chim. Acta 1058, 9–17.
Oliveri, P., Malegori, C., Casale, M., 2020. Chemometrics: multivariate analysis of chemical data. In: Pico, Y. (Ed.), Chemical Analysis of Food, 2nd edition Elsevier.
Ordóñez, A., Silva, V., Galán, P., Loredo, J., Rucandio, I., 2014. Arsenic input into the catchment of the River Caudal (Northwestern Spain) from abandoned Hg mining works: effect on water quality. Environ. Geochem. Health 36, 271–284.
Petranich, E., Croce, S., Crosera, M., Pavoni, E., Faganeli, J., Adami, G., Covelli, S., 2018. Mobility of metal(loid)s at the sediment-water interface in two tourist port areas of the Gulf of Trieste (northern Adriatic Sea). Environ. Sci. Pollut. Res. 25, 26887–26902.
Pfeifle, B.D., Stamm, J.F., Stone, J.J., 2018. Arsenic geochemistry of alluvial sediments and pore waters affected by mine tailings along the Belle Fourche and Cheyenne River floodplains. Water Air Soil Poll 229, 183.
Ridgway, J., Shimmield, G., 2002. Estuaries as repositories of historical contamination and their impact on shelf seas. Estuar. Coast. Shelf Sci. 55, 903–928.
Roberts, D.A., 2012. Causes and ecological effects of resuspended contaminated sediments (RCS) in marine environments. Environ. Int. 40, 230–243.
Rodríguez Martin-Doimeadios, R.C., Monperrus, M., Krupp, E., Amouroux, D., Donard, O.F.X., 2003. Using speciated isotope dilution with GC— inductively coupled plasma MS to determine and unravel the artificial formation of monomethylmercury in certified reference sediments. Anal. Chem. 75, 3202–3211.
Rodríguez-González, P., Ruiz Encinar, J., García Alonso, J.I., Sanz-Medel, A., 2002. Determination of butyltin compounds in coastal sea-water samples using isotope dilution GC-ICP-MS. J. Anal. Atom. Spectrom. 17, 824–830.
Rodríguez-González, P., Monperrus, M., García Alonso, J.I., Amouroux, D., Donard, O.F.X., 2007. Comparison of different numerical approaches for multiple spiking species-specific isotope dilution analysis exemplified by the determination of butyltin species in sediments. J. Anal. Atom. Spectrom. 22, 1371–1382.
Rodríguez-González, P., Bouchet, S., Monperrus, M., Tessier, E., Amouroux, D., 2013. In situ experiments for element species-specific environmental reactivity of tin and mercury compounds using isotopic tracers and multiple linear regression. Environ. Sci. Pollut. R. 20, 1269–1280.
Root, R.A., Dixit, S., Campbell, K.M., Jew, A.D., Hering, J.G., O'Day, P.A., 2007. Arsenic sequestration by sorption processes in high-iron sediments. Geochim. Cosmochim. Ac. 71, 5782–5803.
Ruiz-Chancho, M.J., Sabé, R., López-Sánchez, J.F., Rubio, R., Thomas, P., 2005. New approaches to the extraction of arsenic species from soils. Microchim. Acta 151 (3–4), 241–248.
Sanford, L.P., Panageotou, W., Halka, J.P., 1991. Tidal resuspension of sediments in northern Chesapeake Bay. Mar. Geol. 97, 87–103.
Sanz-Prada, L., García-Ordiales, E., Roqueñi, N., Grande Gil, J.A., Loredo, J., 2020. Geochemical distribution of selected heavy metals in the Asturian coastline sediments. Mar. Pollut. Bull. 156, 111263.
Saulnier, I., Mucci, A., 2000. Trace metal remobilization following the resuspension of estuarine sediments: Saguenay Fjord, Canada. Appl. Geochem. 15, 191–210.
Schoellhamer, D.H., 1996. Anthropogenic sediment resuspension mechanisms in a shallow microtidal estuary. Estuar. Coast. Shelf Sci. 43, 533–548.
Seelen, E.A., Massey, G.M., Mason, R.P., 2018. Role of sediment resuspension on estuarine suspended particulate mercury dynamics. Environ. Sci. Technol. 52, 7736–7744.
Shepard, F.P., 1954. Nomenclature based on sand–silt–clay ratios. J. Sediment. Petrol. 24, 151–158.
Silva, V., Loredo, J., Fernández-Martínez, R., Larios, R., Ordóñez, A., Gómez, B., Rucandio, I., 2014. Arsenic partitioning among particle-size fractions of mine wastes and stream sediments from cinnabar mining districts. Environ. Geochem. Health 36, 831–843.
Simpson, S.L., Apte, S.C., Batley, G.E., 1998. Effect of short-term resuspension events on trace metal speciation in polluted anoxic sediments. Environ. Sci. Technol. 32, 620–625.
Smedley, P.L., Kinniburgh, D.G., 2002. A review of the source, behaviour and distribution of arsenic in natural waters. Appl. Geochem. 17, 517–568.
Stephens, S.R., Alloway, B.J., Parker, A., Carter, J.E., Hodson, M.E., 2001. Changes in the leachability of metals from dredged canal sediments during drying and oxidation. Environ. Pollut. 114, 407–413.
Symons, D.T.A., Kawasaki, K., Tornos, F., Velasco, F., Rosales, I., 2017. Temporal constraints on genesis of the Caravia-Berbes fluorite deposits of Asturias, Spain, from paleomagnetism. Ore Geol. Rev. 80, 754–766.
Turner, A., Millward, G.E., Le Roux, S.M., 2004. Significance of oxides and particulate organic matter in controlling trace metal partitioning in a contaminated estuary. Mar. Chem. 8, 179–192.
Van Den Berg, G.A., Meijers, G.G.A., Van Der Heijdt, L.M., Zwolsman, J.J.G., 2001. Dredging-related mobilisation of trace metals: a case study in the Netherlands. Water Res. 35, 1979–1986.

Vidal-Durà, A., Burke, I.T., Stewart, D.I., Mortimer, R.J.G., 2018. Reoxidation of estuarine sediments during simulated resuspension events: effects on nutrient and trace metal mobilisation. Estuar. Coast. Shelf Sci. 207, 40–55.
Wang, H., Liu, R., Wang, Q., Xu, F., Men, C., Shen, Z., 2016. Bioavailability and risk assessment of arsenic in surface sediments of the Yangtze River estuary. Mar. Pollut. Bull. 113, 125–131.
Wilkin, R.T., Ford, R.G., 2006. Arsenic solid-phase partitioning in reducing sediments of a contaminated wetland. Chem. Geol. 228, 156–174.
Zhu, W., Song, Y., Adediran, G.A., Jiang, T., Reis, A.T., Pereira, E., Skyllberg, U., Björn, E., 2018. Mercury transformations in resuspended contaminated sediment controlled by redox conditions, chemical speciation and sources of organic matter. Geochim. Cosmochim. Ac. 220, 158–179.